Sustainable Energy & Fuels

ROYAL SOCIETY OF CHEMISTRY

PAPER

View Article Online
View Journal | View Issue

Cite this: *Sustainable Energy Fuels*, 2021, **5**, 3687

Hydrocarbon-based Pemion™ proton exchange membrane fuel cells with state-of-the-art performance†

Hien Nguyen, [ab] Florian Lombeck,[b] Claudia Schwarz,[ab] Philipp A. Heizmann, [a] Michael Adamski,[c] Hsu-Feng Lee, [c] Benjamin Britton, [c] Steven Holdcroft,[d] Severin Vierrath [ab] and Matthias Breitwieser*[ab]

Non-fluorinated hydrocarbon ionomers feature distinct technical, cost, and environmental advantages over incumbent perfluorinated sulfonic acid (PFSA)-based ionomers: they offer improved thermo-mechanical properties at temperatures beyond 90 °C, likelihood of lower material cost, lower gas cross-over, and facile recycling of platinum group metals. In addition, fluorine-free hydrocarbon ionomers are less hazardous to the environment owing to the lack of (per)fluorinated precursors. Yet, the performance of hydrogen fuel cells with hydrocarbon-based ionomers and membranes has been historically largely inferior to the PFSA-based state of the art. In this study, we present wholly hydrocarbon fuel cells exceeding previous literature landmarks by a factor of nearly two, with peak power densities of 2.1 W cm^{-2} under H_2/O_2 (atmospheric pressure and 95% relative humidity), and 1.1 W cm^{-2} under H_2/air (250 kPa_{abs} and 50% relative humidity). This improvement was achieved by the use of Pemion™ – a sulfo-phenylated polyphenylene-based cation exchange material – as ionomer in the catalyst layer and as proton exchange membrane with a low thickness of 7 μm, and an optimization of cathode catalyst layer based on PtCo/C. Based on an in-depth study of electrochemical performance under various conditions *vs.* a state-of-the-art PFSA reference cell, the performances of Pemion™-based cells were found to be more sensitive to changes in relative humidity of inlet gases, but the detrimental influence of high temperatures on performance was significantly reduced. At an operation temperature of 110 °C, 250 kPa_{abs}, and 50% relative humidity, the peak power density (0.96 W cm^{-2}) was 8% higher than the short-side chain PFSA-based reference cell (0.89 W cm^{-2}), highlighting the potential of Pemion™ for next-generation fuel cells for heavy-duty or aeronautic applications.

Received 13th April 2021
Accepted 18th June 2021

DOI: 10.1039/d1se00556a

rsc.li/sustainable-energy

1 Introduction

The operation of modern electrochemical energy conversion devices, such as hydrogen fuel cells and water electrolyzers, is facilitated in-part by a solid-state polymer electrolyte, which serves as both an electrode-separating membrane, and ionomer (or "binder") in the catalyst layer (CL). Since the 1960s, the technological benchmark of such materials has been a proton-conducting perfluorinated sulfonic acid (PFSA) ionomer, such as Nafion™, and more recently short-side chain (SSC) and/or derivatives thereof, such as Aquivion™, Flemion™ or Hyflon™.[1] Yet, PFSAs feature several drawbacks which include: (1) environmental hazards associated with the use of (per) fluorinated compounds and their recovery,[2,3] (2) high costs, both as a result of complex chemical processes and globally-restricted manufacturing; and (3) a limited operating temperature range due to the unsatisfactory thermo-mechanical properties at temperatures beyond 90 °C.[4,5] Consequently, the pursuit of alternative hydrocarbon-based ionomer chemistries and materials solutions has attracted measurable attention from academia and industry alike,[6–8] especially since fuel cell operation temperatures in the range of 100 °C–120 °C have become the official targets set by the Japanese New Energy Development Organization (NEDO)[9] and by the U.S. Department of Energy (DOE).[10] At elevated temperatures (>100 °C) reaction kinetics are enhanced, heat and water management in the fuel cell systems is simplified, and the effect of impurities in hydrogen causing catalyst poisoning are mitigated.[11–14] However, operating a fuel cell at temperatures higher than 100 °C creates significant issues, especially for Nafion™-type ionomers. Most important challenges are the dehydration of the

[a]*Electrochemical Energy Systems, IMTEK – Department of Microsystems Engineering, University of Freiburg, Georges-Koehler-Allee 103, 79110 Freiburg, Germany. E-mail: matthias.breitwieser@imtek.de*

[b]*Hahn-Schickard, Georges-Koehler-Allee 103, 79110 Freiburg, Germany*

[c]*Ionomr Innovations Inc., 111-2386 East Mall, Vancouver, BC V6T 1Z3, Canada*

[d]*Department of Chemistry, Simon Fraser University, Burnaby, BC V5A 1S6, Canada*

† Electronic supplementary information (ESI) available. See DOI: 10.1039/d1se00556a

membrane and electrode ionomer, with a subsequent decrease in proton conductivity, accelerated gas crossover, and exacerbated membrane degradation processes.[4,14,15] However, the fact that the thermo-mechanical properties of hydrocarbon polymers are not affected by temperatures beyond 90 °C has renewed interest in hydrocarbon-based polymer electrolytes in recent years.

Functionalized polyaromatic ionomers represent the largest class of hydrocarbon-based polymer electrolytes investigated to date, due in-part to the enhanced thermochemical resilience associated with sp^2–sp^2 chemical linkages *versus* those of sp^3–sp^3 linkages found on early polyvinyl-based structures.[7,11,16] Nevertheless, a persistent criticism of these materials is in their lack of chemical and mechanical durability, and generally poorer performance evaluated in hydrogen fuel cells, compared to their PFSA counterparts.[17,18] Recently, a focus on the development of hydrocarbon-based polymer electrolytes encompassing long-term *in situ* durability together with *ex situ* and *in situ* electrochemical performance has yielded promising alternatives to incumbent PFSAs. A common polymer architecture employed in such materials is the polyphenylene backbone, which unlike preceding poly(arylene ether)s and numerous derivatives thereof, contain no backbone linkages particularly susceptible to chemical degradation.[1] For example, Skalski *et al.*,[19] Adamski *et al.*,[20] Miyake *et al.*,[21] Shiino *et al.*,[22] Xu *et al.*,[23] and Shimizu *et al.*,[24] reported PEMs with best-in-class chemical durability, all based on a polyphenylene backbones. Compared to PFSAs, however, the reported *ex situ* and *in situ* durabilities of hydrocarbon polyphenylene-based PEMs have been contradictory. Although the rate constant of reaction of the primary degradative species in hydrogen fuel cells, the $HO^{\bullet}$ radical, is approx. 10^3 times greater for polyphenylene,[25] the *in situ* lifetime of polyphenylene PEMs is >3× greater when evaluated in an open circuit voltage (OCV) accelerated stress test (AST) using the DOE protocol.[20,23]

In terms of *ex situ* electrochemical characteristics, numerous polyphenylene-based membranes exhibit measurably greater proton conductivity than PFSAs such as Nafion 211 at high humidity. At low humidity, however, proton conductivity declines disproportionately due to a greater dependence on water content on proton conduction. This is primarily due to the different density between sulfonated polyphenylenes and related polyaromatic hydrocarbons (typically in the range of 1.3 g cm^{-3}),[26] *versus* that of PFSAs (*e.g.* 1.9 g cm^{-3} for Nafion[27]), as the polymer repeat unit in perfluorinated materials possesses a higher weight than in hydrocarbon-based materials. Thus, the volumetric density of protonic sites is lower for hydrocarbon ionomers at the same IEC.[28] Consequently, hydrocarbon-based PEMs typically require a significantly higher amount of acid functional groups per repeat unit (>2×), and hence a greater ion exchange capacity (IEC), approx. 2 mmol g^{-1} and above, to achieve similar protonic conductivity to PFSAs. The higher IEC imparts increased hydrophilicity, and as a result, potentially excessive water sorption, swelling, when fully hydrated. Another reason for the lower proton conductivity with decreasing water content is the reduced connectivity of the hydrophilic domains.[29,30] In addition, the acidity of aryl sulfonic acid groups ($pK_a \sim -1$) is measurably lower than the acidity of superacidic perfluorosulfonic acid groups ($pK_a \sim -6$).[29,31] The degree of dissociated acid is hence compromised under very low humidity (<10%).[32]

In terms of *in situ* fuel cell performance, even highly conducting polyphenylene-based membranes typically yield poorer performance, due to complex relationships between the polymer's protonic conductivity, water content and swelling, and compromised mechanical integrity, the impacts of which are amplified when humidity is subsequently reduced or cycled.[20,21,33] Under variable load conditions, corresponding to hydrothermal cycles and membrane swelling–deswelling, the risk of mechanical failure of the membrane is thereby greatly increased. Using hydrocarbon-based ionomers in catalyst layers typically leads to inferior performance compared to PFSA-based materials. The inferior performance of such wholly hydrocarbon fuel cells is typically attributed to slower kinetics, lower electrochemically active surface area (ECSA), reduced proton conductivity at low humidity or poor oxygen transport through the ionomer film and/or reduced porosity at high humidity.[2,34,35]

Nonetheless, progress has been made with polyphenylene-based ionomers demonstrating their increasing viability of use. Skalski *et al.*[36] reported a series of membrane electrode assemblies (MEAs) yielding peak power densities of 770 mW cm^{-2} under H_2/O_2 and 456 mW cm^{-2} under H_2/air (both at 95% RH and ambient pressure). Their MEAs contained sulfonated phenylated polyphenylene copolymers sPPP(m)-H^+ as both membrane and ionomer in the catalyst layer. Following this progress, Balogun *et al.*[33] reported MEAs comprising structurally-similar sulfonated phenylated polyphenylene biphenyls sPPB-H^+, which exhibited peak power densities over 1 W cm^{-2} under H_2/O_2, and 677 mW cm^{-2} under H_2/air at 95% RH and ambient pressure. Chae *et al.*[37] reported wholly hydrocarbon MEAs incorporating sulfonated poly(arylene ether sulfone) (sPAES)-based ionomers which exhibited peak power densities of 700 mW cm^{-2} under H_2/air under fully humidified anode and cathode gas feeds.

While the aforementioned reports demonstrate decisive progress with respect to *in situ* performance of hydrocarbon-based MEAs, there remains room for significant improvement compared to PFSA MEAs. For example, peak power densities of PFSA MEAs commonly exceed peak powder densities of 1.4 W cm^{-2} under H_2/O_2 at 95% RH and ambient pressure.[33,38] Hence, despite several promising features, there remain underlying drawbacks in current hydrocarbon, polyphenylene-based materials. Namely, poor *in situ* performance, particularly under reduced RH and thus operationally relevant conditions, a strong dependence of electrochemical performance on material hydration, and greater material swelling and dimensional instability.

In this work, we present wholly hydrocarbon MEAs comprising Pemion™, a sulfonated polyphenylene-based PEM (Fig. 1) as both membrane and ionomer in the catalyst layer. PtCo/C was used in the catalyst layer as it was shown in recent publications[39,40] to enable very high mass activities and fuel cell performances. With a peak power density of 2.1 W cm^{-2} under H_2/O_2 (95% RH, 80 °C, ambient pressure), and 1.1 W cm^{-2}

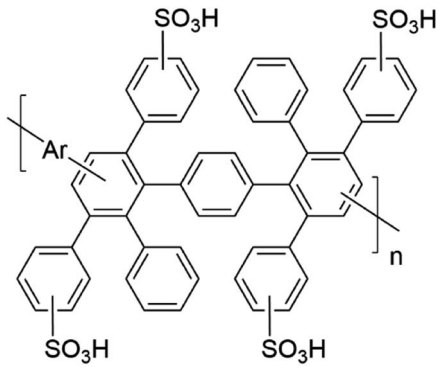

Fig. 1 Structures of Pemion™ – a variation of sulfo-phenylated polyphenylenes (sPPX-H^+).

under H_2/air (80% RH, 80 °C, 250 kPa_{abs}), we significantly exceed all reported values for wholly hydrocarbon fuel cells, and for the first time reach performance comparable to state-of-the-art PFSA-based fuel cells. The work includes in-depth characterization at industrially relevant operational conditions (hot and dry) and presents stable operation beyond 100 °C.

2 Experimental

Pemion™ PP1-HNN9-00-X ionomer and Pemion™ PF1-HNN9-07-X membranes were supplied by Ionomr Innovations, Inc. The materials are the same chemistry and IEC. This and further information is provided in the publicly available specification sheets for both materials. Short-side chain (SSC) PFSA ionomer was supplied by 3M and SSC PFSA FS715RFS membranes were supplied by Fumatech GmbH.

2.1 Preparation of catalyst inks

5 wt% solutions of Pemion™ were prepared in-house with Pemion™ ionomer (IEC = 3.1 meq. g^{-1}, 320 EW) in a mixture of 3 : 1 w/w methanol (MeOH)/water for the anode and 1 : 1 w/w isopropyl alcohol (IPA)/water for the cathode. The Pemion™ solution was treated in an ice bath by sonication with an ultrasonic probe (Hielscher UIS250L) at 100 W for 20 minutes.

Anode catalyst inks (0.95 wt% solids in 3 : 1 w/w MeOH/water) were prepared using Pt/C (45.3 wt% Pt content, Elyst Pt50 0550, Umicore). The catalyst was dispersed in a mixture of 3 : 1 w/w MeOH/water and Pemion™ solution (5 wt% in 3 : 1 w/w MeOH/water). Cathode catalyst inks (0.95 wt% solids in 1 : 1 w/w IPA/water) were prepared using PtCo/C (45.3 wt% Pt content, Elyst Pt50 0690, Umicore). The catalyst was dispersed in a mixture of 1 : 1 w/w IPA/water and Pemion™ solution (5 wt% in 1 : 1 w/w IPA/water). The ionomer content in both anode and cathode catalyst inks was 9 wt% dry which corresponds to an ionomer-to-carbon (I/C) weight ratio of 0.2. All catalyst inks were treated in an ice bath by sonication with an ultrasonic probe (Hielscher UIS250L) at 100 W for one hour.

5 wt% solutions of SSC PFSA were prepared in-house with 3M SSC PFSA ionomer (IEC = 1.3 meq. g^{-1}, 800 EW) in IPA. The PFSA solution was stirred at 60 °C for at least 12 h. Same catalysts were used as in the Pemion™ MEAs, *i.e.*, Pt/C (45.3 wt% Pt content, Umicore) for the anode and PtCo/C (45.3 wt% Pt content, Elyst Pt50 0690, Umicore) for the cathode. The optimized ratio of the IPA/water mixture for the catalyst ink was 1 : 4 w/w. To guarantee a meaningful performance comparison between PFSA and hydrocarbon cells, an optimized ionomer content for the SSC-PFSA reference of 18 wt% dry was used, which corresponds to an I/C ratio of 0.4.

2.2 Fabrication of membrane–electrode assemblies

The catalyst layers were applied onto pristine membranes using an automated ultrasonic spray system (Sonaer Sono-Cell). Pemion™ anode and cathode catalyst inks were applied onto Pemion™ membranes (IEC = 2.9 meq. g^{-1}, 340 EW, nominal thickness: 7 μm). As reference, SSC PFSA anode and cathode catalyst inks were applied onto a thin commercial Fumapem® membranes (IEC = 1.4 meq. g^{-1}, 725 EW, nominal thickness:

Table 1 Experimental protocol used in all experiments

Experimental	Details
Break-in	80 °C, H_2/O_2, 0.25/1 slpm, 95% RH, ambient pressure, OCV – 0.3 V–0.6 V, 20×
O_2 pol curve	80 °C, H_2/O_2, 0.25/1 slpm, 95% RH, ambient pressure
Stabilization	80 °C, N_2 purge, 0.2 slpm, 1 hour, ambient pressure
	35 °C, N_2 purge, 0.2 slpm, 1.5 hours, ambient pressure
HAD[a]	35 °C, H_2/N_2, 0.2/0 slpm, 50 mV s^{-1}, 0.05–1.2 V, ambient pressure, 95% RH, 8×
CV	80 °C, H_2/N_2, 0.2/0 slpm, 50 mV s^{-1}, 0.05–1.2 V, ambient pressure, 30% RH, 8×
	80 °C, H_2/N_2, 0.2/0 slpm, 50 mV s^{-1}, 0.05–1.2 V, ambient pressure, 50% RH, 8×
	80 °C, H_2/N_2, 0.2/0 slpm, 50 mV s^{-1}, 0.05–1.2 V, ambient pressure, 80% RH, 8×
	80 °C, H_2/N_2, 0.2/0 slpm, 50 mV s^{-1}, 0.05–1.2 V, ambient pressure, 95% RH, 8×
Air pol curves	Varied RH, 80 °C, H_2/air, 0.25/1 slpm, 250 kPa absolute, 30% RH/30% RH
	Varied RH, 80 °C, H_2/air, 0.25/1 slpm, 250 kPa absolute, 50% RH/50% RH
	Varied RH, 80 °C, H_2/air, 0.25/1 slpm, 250 kPa absolute, 80% RH/80% RH
Air pol curves	Varied temperatures, 80% RH, H_2/air, 0.25/1 slpm, 250 kPa absolute, 94 °C
	Varied temperatures, 80% RH, H_2/air, 0.25/1 slpm, 250 kPa absolute, 100 °C
Air pol curves	50% RH, H_2/air, 0.25/1 slpm, 250 kPa absolute, 110 °C

[a] Hydrogen adsorption/desorption.

15 μm). The desired Pt-loading of all MEAs was 0.1 mg cm^{-2} and 0.4 mg cm^{-2} for the anode and the cathode, respectively.

2.3 Electrochemical characterization

The resulting catalyst-coated membranes were sandwiched between two 4 cm^2 gas diffusion layers (H14C-Series, Freudenberg). The performances of the 4 cm^2 active area MEAs were evaluated using a fuel cell test station (Scribner 850e). All MEAs were tested with the same experimental protocol. Shown error bars are based on at least two individual MEAs from different production batches to ensure reproducibility of the results. Electrochemical characterization was performed by analysing polarization data and cyclic voltammograms (CV). Table 1 lists the experimental protocol applied in this study.

Conditioning procedures. MEAs were conditioned at 80 °C and 95% RH with inlet gas flows of 0.25 slpm H_2 anode and 1 slpm O_2 cathode. The cell was held at its open circuit voltage, 0.3 V and 0.6 V for 1 minute each. The voltage cycles were repeated 20 times to ensure stable operation.

H_2/O_2 polarization curves. The protocol involved taking measurements over two current density ranges at 80 °C, 95% RH and atmospheric pressure. For Tafel analysis, the current density was scanned from zero to 250 mA cm^{-2} in 12.5 mA cm^{-2} increments with a 1 minute hold for each current step. To generate the full polarization curve, the current density was scanned from 500 mA cm^{-2} to 6250 mA cm^{-2} at 250 mA cm^{-2} increments with a 3 minute hold at each current step. The data point is the average over the last 5 seconds in all polarization

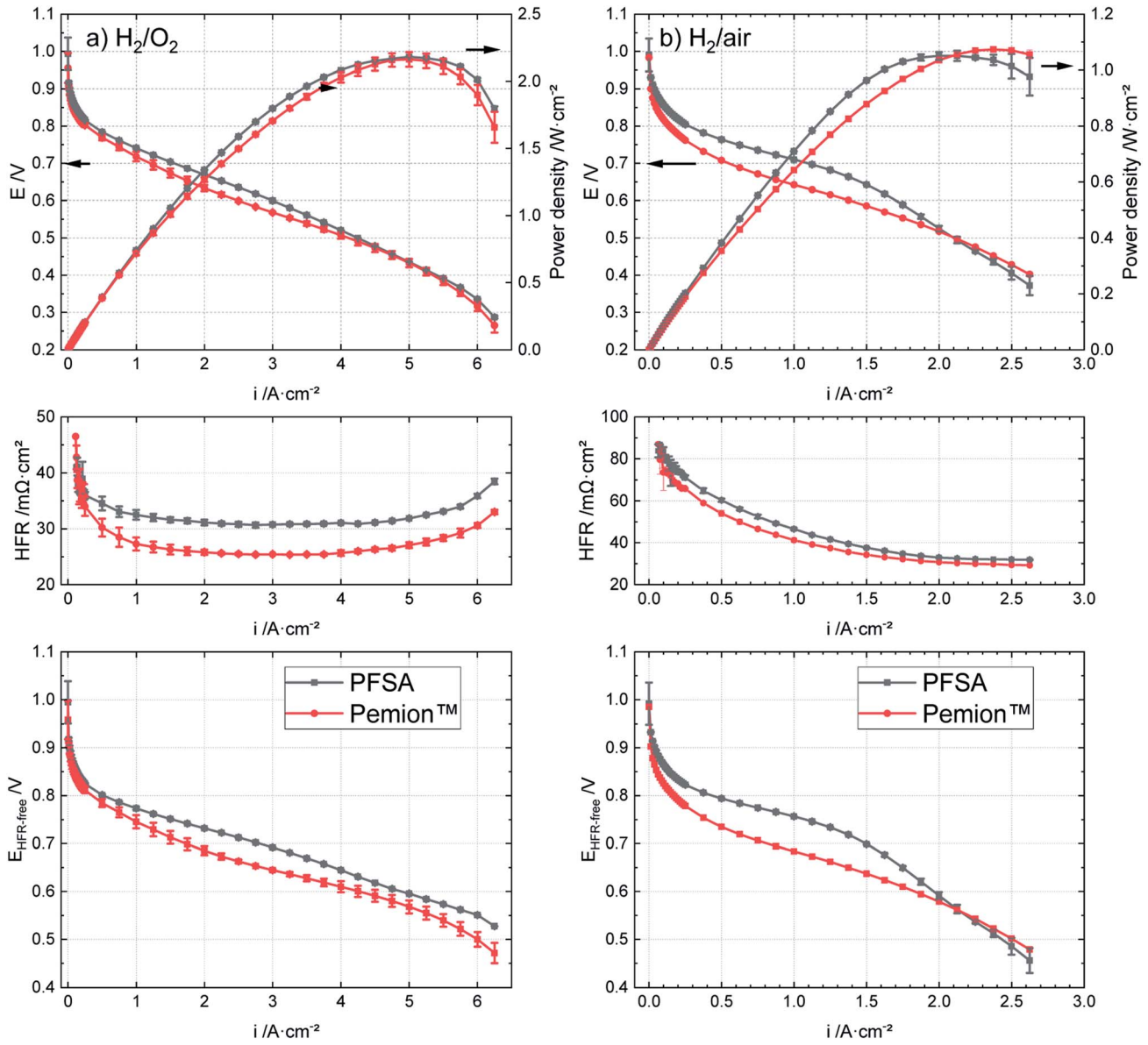

Fig. 2 Polarization behaviours, HFRs and HFR-corrected cell voltages of Pemion™ MEA *vs.* PFSA reference at 80 °C under (a) H_2/O_2, 0.25 slpm/1 slpm, 95% RH and ambient pressure and (b) H_2/air, 0.25 slpm/1 slpm, 50% RH, 250 kPa_{abs}.

curves. The flow rates of H_2 and O_2 at the anode and cathode were 0.25 slpm and 1 slpm, respectively.

Stabilization. The gas feed dew point temperature was cooled down from 79 °C to 34 °C for the later hydrogen adsorption/desorption (HAD) measurement with N_2 purge to avoid flooding of the CLs. After 1 h, the cell was equilibrated at 35 °C in H_2/N_2 for additional 1.5 h. The cathode was purged with 0.2 slpm N_2 to avoid any oxygen reduction currents arising from oxygen residues in the gas lines that would affects the later evaluation of the CV.

Hydrogen adsorption/desorption (HAD). The electrochemical surface area (ECSA) was determined by integrating the area associated with hydrogen adsorption in cyclic voltammograms. CV measurements were conducted under 35 °C and under fully humidified H_2 (0.2 slpm) at the anode and an interrupted N_2 flow at the cathode to avoid artefacts in the ECSA distribution.[41] The potential was swept 8× from 0.05 to 1.20 V at a scan rate of 50 mV s^{-1}. The unit charge was assumed to be 210 μC cm^{-2} for hydrogen adsorption integrated areas in determining ECSA as in other studies with PtCo/C[42,43] even though this historical value contains various assumptions and approximations.[41,44,45]

Cyclic voltammetry (CV). Cyclic voltammograms with symmetrically increasing RH levels were measured at 80 °C and ambient pressure with H_2/N_2 for the anode and cathode, respectively. The flow rates at the anode and cathode were 0.2/0 slpm, respectively. The potential was swept 8× from 0.05 to 1.20 V at a scan rate of 50 mV s^{-1} until saturation was reached. Shown cyclic voltammograms were obtained from the last potential sweep.

H_2/air polarization curves. H_2/air polarization curves with symmetrically increasing RH levels (30%, 50%, and 80%) were measured at 80 °C and 250 kPa_{abs} for both anode and cathode. The measurements started at low RH to ensure the validity of polarization curves with lower humidity, as rest water from previous experiment with higher humidity could remain in the CLs and affect the cells at lower humidity level positively. H_2/air polarization curves with increasing cell temperatures (94 °C, 100 °C) were measured at 80% RH and 250 kPa_{abs}, also for both anode and cathode. H_2/air polarization curves at 110 °C were measured at 50% RH and 250 kPa_{abs} for both anode and cathode. Similar to the scan current experiment for H_2/O_2 polarization curves, the protocol started to measure from zero to 250 mA cm^{-2} in 12.5 mA cm^{-2} increments with a 1 minute hold at each current step. Full polarization curves were generated by scanning the current density from 375 mA cm^{-2} to 6250 mA cm^{-2} in 125 mA cm^{-2} increments with a 3 minute hold at each current step. The flow rates of H_2 and air at the anode and cathode were 0.25 slpm and 1 slpm, respectively.

High frequency resistances (HFRs) were measured at a frequency of 3200 Hz by the fuel cell test station's integrated Frequency Resistance Analyzer (FRA) throughout all polarization characterizations and used to correct for membrane, contact, and electronic resistances.

The cross section of the Pemion™ MEA and the morphology of the cathode catalyst layers of both MEAs was characterized by field emission-scanning electron microscopy (Tescan Amber X) at an acceleration voltage of 2 keV and a beam current of 100 pA. The working distance was 6 mm. SEM micrographs and additional information regarding the HAD measurement and cyclic voltammogramms under varied RH are presented in the ESI.†

3 Results and discussion

The ionomer contents in the electrodes were optimized for a fully humidified H_2/O_2 gas feed. The optimal ionomer content was found to be lower for the Pemion™ MEA (9 wt%) than for the reference PFSA MEA (18 wt%) which is in accordance with the trends in literature.[33,46] For more information the reader is directed to the ESI (Fig. S1).†

3.1 *I–V* performance

The polarization curves of Pemion™ and PFSA MEAs under H_2/O_2 and in H_2/air are shown in Fig. 2. In general, the *I–V* performance of the wholly hydrocarbon MEA under H_2/O_2 is comparable to that of the PFSA reference (Fig. 2a). The peak power density of the Pemion™ MEA in oxygen (2.1 W cm^{-2}) is similar to that of the PFSA reference (2.2 W cm^{-2}).

Fig. 3 illustrates the performance trends of fully hydrocarbon MEAs from 2008. The developed hydrocarbon materials have been based on SPEEK,[34] SPAES,[35] or sulfonated poly(-phenylene).[36,38] The performance of the Pemion™ MEA exceeds previous wholly hydrocarbon MEAs literature landmarks, by a factor of nearly two with peak power densities of 2.1 W cm^{-2} under H_2/O_2, 95% RH and ambient pressure.

While there are not many commercial hydrocarbon ionomers available on the market (only NEXAR™ is known in literature[47,48] and Pemion™ was introduced in this work), a plenty of studies on hydrocarbon ionomers can be found in

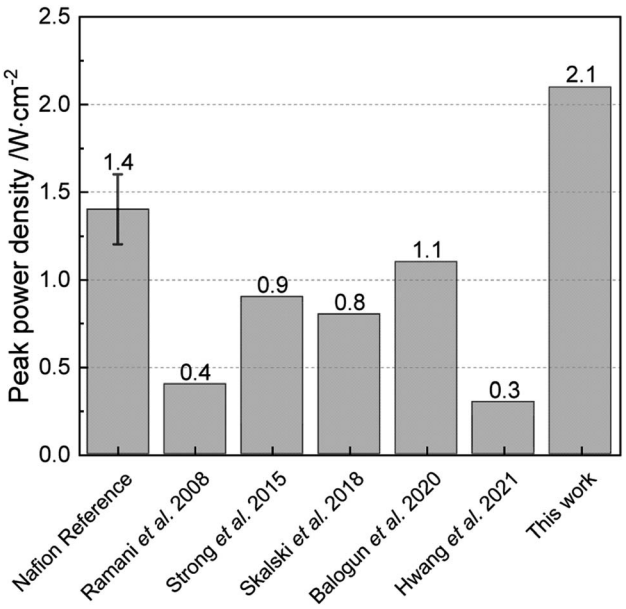

Fig. 3 Peak power densities of fully hydrocarbon MEAs over the last decades under the same conditions: 80 °C, H_2/O_2, high humidity (>75% RH) and ambient pressure.[33–36,47]

Table 2 Tafel slopes in the kinetic region (25–100 mA cm^{-2}) extracted from the HFR-corrected curves of all MEAs under H_2/O_2 (0.25 slpm/1 slpm), 95% RH and ambient pressure

Samples	PtCo + Pemion™	PtCo + PFSA
Tafel slope in mV dec^{-1}	74	73
Mass activity in A mg_{Pt}^{-1} at 900 $mV_{HFR\text{-}free}$	0.056	0.074

literature in the last decades. The work of Holdcroft, Kreuer and Miyatake are the most well-known ones in developing hydrocarbon (membrane) ionomers for low to mid-temperature fuel cells (<150 °C) to-date and have published many articles on benchmark hydrocarbon-based MEAs.[6,33,49,50]

Not shown in Fig. 3 is, for instance, the excellent work of Long *et al.*[50] with sulfonated poly(phenylene) containing additional tetrafluorophenylene groups in the membrane, but with Nafion™ as electrode electrolyte. The power density at 0.6 V was 0.9 W cm^{-2}, which is higher than the to-date reported fully hydrocarbon cells (0.7 W cm^{-2}) at the same potential.[33] The peak power density of the MEA was not reported. Also the excellent work of Kreuer and co-workers[28,70] with the 10 μm sulfonated polysulfone (S360) with PBIOO blend membrane (peak power density > 2.5 W cm^{-2} under H_2/O_2 and 95% RH and

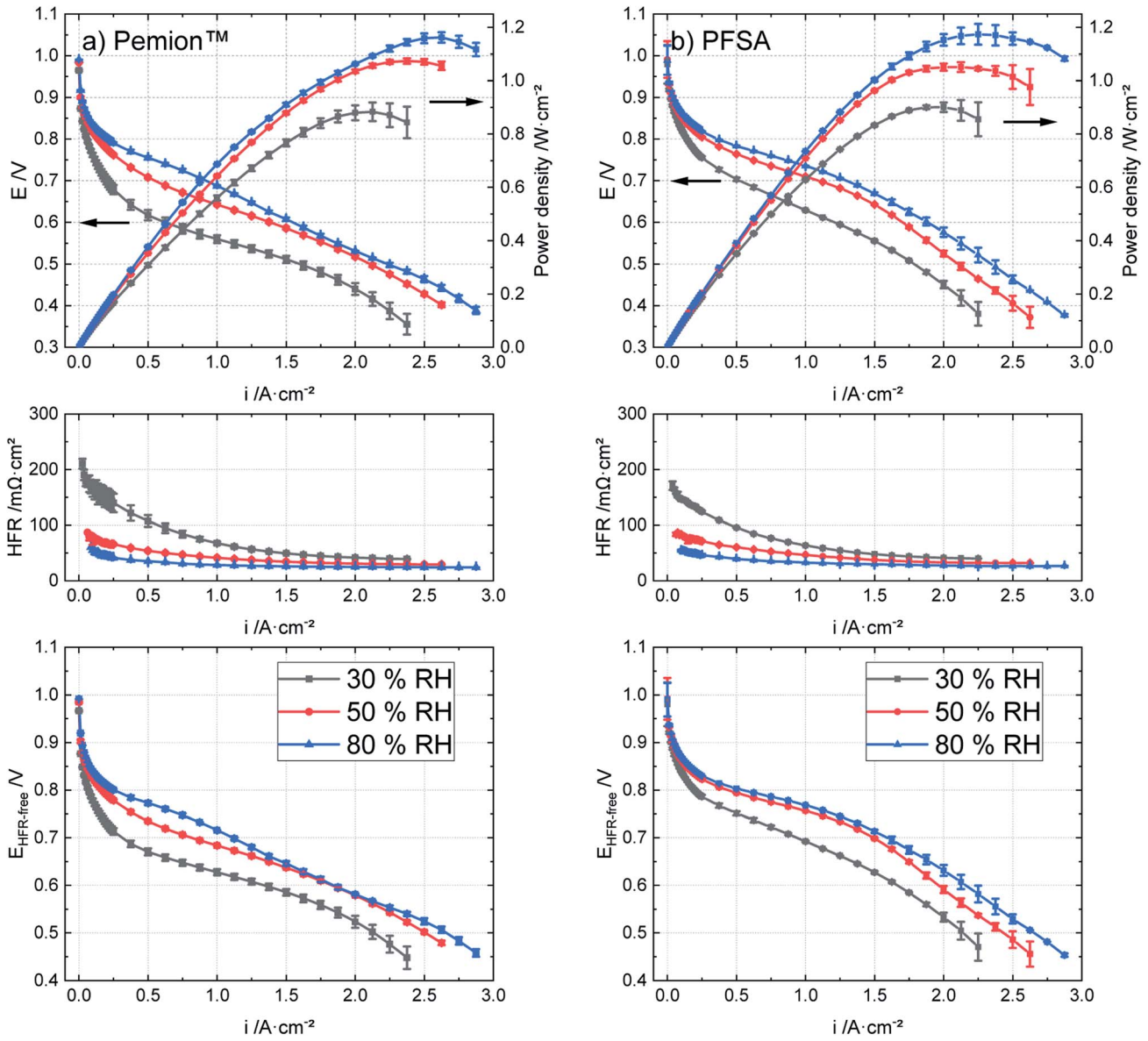

Fig. 4 Polarization behaviours, HFR and HFR-corrected cell voltages of (a) Pemion™ MEA and (b) PFSA reference under varied RH levels at 80 °C, H_2/air, 250 kPa_{abs}.

300 kPa_{abs}) is not comparable with this work (H_2/O_2 and 95% RH and 101 kPa_{abs}) due to the different pressure.

Under automotive-relevant operating conditions (H_2/air, 50% RH and 250 kPa_{abs}), as shown in Fig. 2b, the peak power density of the Pemion™ MEA is similar to that of PFSA reference (~1.1 W cm^{-2}). However, at a potential relevant for automotive applications of 0.6 V, the power density of the Pemion™ MEA (0.83 W cm^{-2}) is still ~20% lower than that of the PFSA reference (1.0 W cm^{-2}). Nonetheless, this is the first hydrocarbon work to be comparable to SSC PFSA in automotive conditions.

In the following, the polarization curves under H_2/O_2 of the two MEAs are discussed in detail to assess the possible loss contributions. Firstly, the high frequency resistance (HFR) of the Pemion™ membrane is approx. 5 mΩ cm^2 lower than that of the PFSA membrane, which is attributed to the lower membrane thickness and the significantly higher ion exchange capacity (IEC) of Pemion™. In order to compare the overpotential losses from the electrodes, the potential losses due to HFR are added to the cell voltage to obtain the HFR-corrected cell voltage $E_{HFR\text{-}free}$. As the overpotential losses due to the hydrogen oxidation reaction and the protonic resistance in the anode can be neglected,[51,52] $E_{HFR\text{-}free}$ mainly consists of the overpotentials related to mass transport, the protonic resistance and to the oxygen reduction reaction in the cathode CL.[52–54]

For pure reactants (under 0.25 slpm/1 slpm H_2/O_2), the mass transport losses are assumed to be negligible at low current densities.[52,54] At the given operating conditions (80 °C, 95% RH, ambient pressure), the proton resistance of the SSC-PFSA ionomer in the reference (0.1 Ω cm^2) is lower than that of LSC-Nafion™-type ionomers (~0.3 Ω cm^2),[38,54,55] as expected due to the higher IEC of the SSC-PFSA ionomer. The proton resistance of Pemion™ ionomer in the CL is 0.5 Ω cm^2, which is higher than that of PFSA ionomers despite the higher IEC of Pemion™ ionomer. The lower proton conductivity of Pemion™ ionomer is most probably due to the lower ionomer-to-carbon (I/C) ratio of the Pemion™ MEA, the less pronounced hydrophilic/hydrophobic phase separation[5,56] and the higher pK_a value of hydrocarbon ionomers compared to PFSA ionomers.[29,31] The conditions and results of the proton impedance measurements are shown in Fig. S2.†

Table 2 shows the Tafel slopes and the mass activities of the Pemion™ MEA and of the PFSA reference. The Tafel slopes of the two MEAs were extracted in the Tafel region between 25 mA cm^{-2} and 100 mA cm^{-2} and plotted with $E_{HFR\text{-}free}$ under H_2/O_2 *vs.* log of crossover-corrected current density $i + i_x$ (see Fig. S3†) following the approach of Gasteiger *et al.*[52,57] The Tafel slopes of the Pemion™ and the PFSA MEA are similar and in accordance with Tafel slopes reported in literature for MEAs with PFSA-based ionomers (~70 mV dec^{-1}).[39,52] While this is expected for the same catalyst, the Tafel slope of our Pemion™ MEA is considerably lower than typical values for hydrocarbon MEAs found in literature,[46,58,59] which shows the progress towards higher kinetic performance.

The mass activity of the Pemion™ MEA is still lower than that of PFSA MEA, indicating a reduced functionality of the active sites in the Pemion™ MEA. Although the precise reason for this reduction of active sites still remains unclear, we hypothesize several possible causes: the significantly lower I/C in the Pemion-based MEA may have a negative impact on mass activity due to a less favourable pronounced triple phase boundary at very low ionomer content. Secondly, as observed for PFSA, it could be related to anion adsorption due to the higher IEC of Pemion™.[60] Third, adsorption of the phenyl groups in Pemion™ on the catalyst surface that poison the catalyst could be a viable explanation. Phenyl poisoning was predicted with DFT calculations and observed in phenyl-based anion-exchange membrane fuel cells and electrolyzers.[61–64] Future work therefore requires the thorough build-up of more understanding of hydrocarbon ionomer/platinum interactions to finally close the herein observed mass activity gap between hydrocarbon and PFSA ionomers.

3.2 The effect of relative humidity on performance

Fig. 4 shows the polarization behaviour of Pemion™ and PFSA MEAs at different levels of humidification (80 °C, H_2/air and 250 kPa_{abs}). Both MEAs show lower performance with decreasing humidity. As mentioned in the experimental section, the humidity was decreased symmetrically in the cathode and anode in this study. In common fuel cell systems for automotive application, however, hydrogen is being recirculated,[65] leading to a higher humidity at the anode and in turn to a reduced effect on performance.[66,67]

At 50% RH, the peak power density of the Pemion™ MEA was similar to PFSA reference (1.10 W cm^{-2}), as discussed in the previous section. With 80% RH, both peak power densities increase by ~5%, for the Pemion™ MEA (1.16 W cm^{-2} at 2.5 A cm^{-2}) and for the PFSA reference (1.17 W cm^{-2} at 2.3 A cm^{-2}). At 30% RH, the peak power density of Pemion™ MEA (0.78 W cm^{-2} at 1.9 A cm^{-2}) is reduced by ~30%, while the peak power density of the PFSA reference (0.90 W cm^{-2} at 2.0 A cm^{-2}) is only ~20% lower compared to 50% RH. These

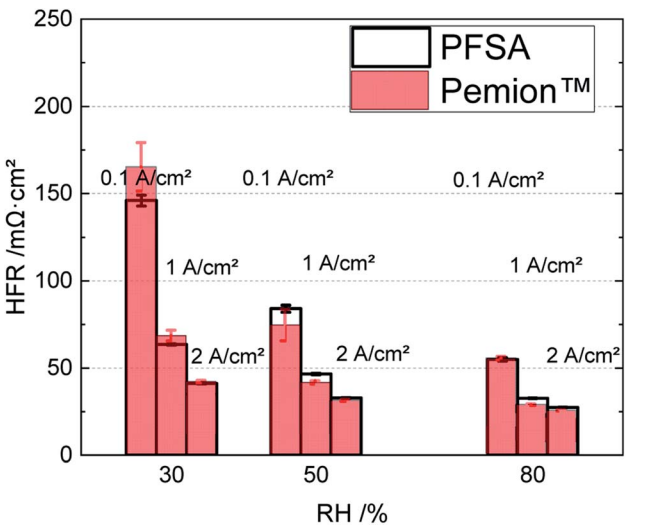

Fig. 5 Direct comparison of the HFRs of Pemion™ MEA and PFSA reference MEA at different current densities (0.1 A cm^{-2}, 1 A cm^{-2} and 2 A cm^{-2}) under varied RH levels (30%, 50% and 80%).

results show that relative humidity has a slightly stronger effect on the performance of the Pemion™ MEA.

Fig. 5 illustrates a direct comparison between the high frequency resistances (HFRs) of both MEAs at three different current densities (0.1 A cm^{-2}, 1 A cm^{-2} and 2 A cm^{-2}) representing the kinetic, ohmic and mass transport region of a polarization curve. Since all components contributing to the electric resistances are identical for both fuel cells, the differences in the HFRs mainly reflect the difference in proton resistance of the membranes. It can be observed that the Pemion™ MEA features a higher HFR under dry conditions (30% RH) in the kinetic region (0.1 A cm^{-2}) but only slightly higher HFR in the ohmic region. At a higher current density (2 A cm^{-2}) and in medium to high humidity levels (50% and 80% RH) the HFR of the Pemion™ MEA is comparable or lower than that of the PFSA reference indicating sufficient membrane humidification. It could be that the slightly lower thickness of Pemion™ membrane compared to the PFSA reference favours back diffusion of water from the cathode to the anode side reducing the HFR at high current density operation (>1 A cm^{-2}), in particular under lower RH.

However, as can be observed in Fig. 4, the HFR-free performance of the PFSA reference is still better than that of the Pemion™ MEA. This indicates that the dependency on gas feed humidity of the Pemion™ MEA performance is not primarily rooted in the PEM but also in the catalyst layers. Several effects could potentially explain this result. Initially, due to the stronger humidity dependency of the hydrocarbon-based Pemion™ ionomers, the proton conductivity of Pemion™ ionomers in the CLs is reduced more significantly in dry conditions.[5,51,54] As the humidity is reduced, less oxide formation (Pt–OH) or other effects such as ionomer surface structuring could potentially reduce the Pt electrochemical active surface area.[51,59,68] These effects might be more severe in Pemion™ MEAs than in PFSA MEAs. For more

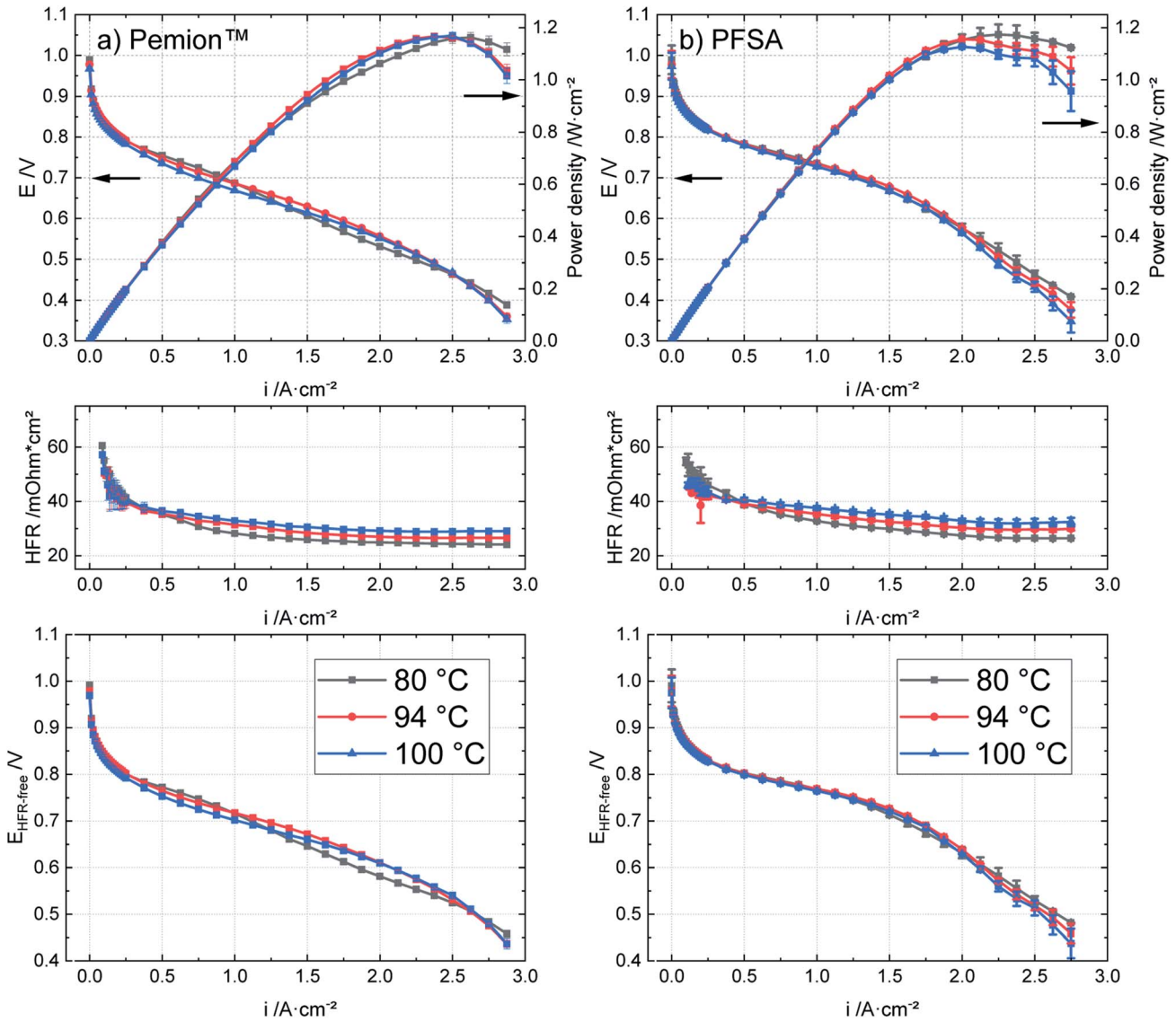

Fig. 6 Polarization behaviours, HFR and HFR-corrected cell voltages of (a) Pemion™ MEA and (b) PFSA reference MEA under 80 °C, 94 °C and 100 °C at 80% humidified H_2/air, 250 kPa_{abs}.

information, the reader is directed to the cyclic voltammograms in the ESI (Fig. S5).†

3.3 High temperature operation

The targeted operating temperature for fuel cell stacks in automotive applications is up to 120 °C.[9,10] Operating at high temperatures leads to numerous benefits such as faster reaction kinetics, diminished impact of impurities in the hydrogen gas feed causing catalyst poisoning, and improved water and heat management in the fuel cell systems.[11–14] On the basis of a so-called heat rejection limit $\frac{Q}{\Delta T}$ the nominal cell voltage is selected in automotive applications. The limit set by U.S. Department of Energy (DOE) is below 1.45 kW K^{-1}.[10] Using eqn (S1)† the rated cell voltage for temperatures from 80 °C to 120 °C can be calculated. For example, at 80 °C cell potentials larger than 0.76 V can meet this heat rejection limit, while increasing the operating temperature to 120 °C allows the rated cell voltage to be as low as 0.55 V (Table S1†). Thus, at higher cell voltages, higher power densities can be obtained if the detrimental influence of high temperatures on performance can be reduced. In the following section, the polarization behaviour of Pemion™ and PFSA MEAs was investigated at temperatures 80 °C–100 °C at a constant relative humidity of 80%. In addition, we give a perspective on performance at temperatures beyond 100 °C.

Fig. 6 shows the performance of Pemion™ and PFSA reference MEAs at different operating temperatures. As the cell temperature is elevated from 80 °C to 100 °C, the overall performance of the PFSA reference decreases by ~5% at current densities above 2 A cm^{-2}. Similar to its PFSA counterpart, the rise in temperature from 80 °C to 100 °C does not appreciably affect the performance of the Pemion™ MEAs. The maximum cell performance of Pemion™ and PFSA MEAs are similar at 94 °C (~1.2 W cm^{-2}) and at 100 °C (~1.1 W cm^{-2}). However, at higher cell potentials > 0.6 V, the PFSA reference outperforms the Pemion™ MEA. For instance, at 94 °C, the rated power density of Pemion™ MEA (0.76 W cm^{-2}) is ~25% lower than PFSA reference (1.0 W cm^{-2}). At 100 °C, the rated power density of Pemion™ MEA (0.80 W cm^{-2}) is also ~25% lower than PFSA reference (1.1 W cm^{-2}) since the performance of both MEAs does not change as the temperature is elevated to 100 °C.

Fig. 7 shows a direct comparison between the HFRs of both MEAs at three different current densities (0.1 A cm^{-2}, 1 A cm^{-2} and 2 A cm^{-2}) as in Fig. 5 in Section 3.2. It can be observed that the HFR of the Pemion™ MEA is higher at 94 °C and 100 °C in the kinetic region (0.1 A cm^{-2}) but lower than PFSA reference in the ohmic region indicating insufficient membrane humidification at low current densities. Overall, the HFRs of both membranes increase slightly as the temperature is elevated but

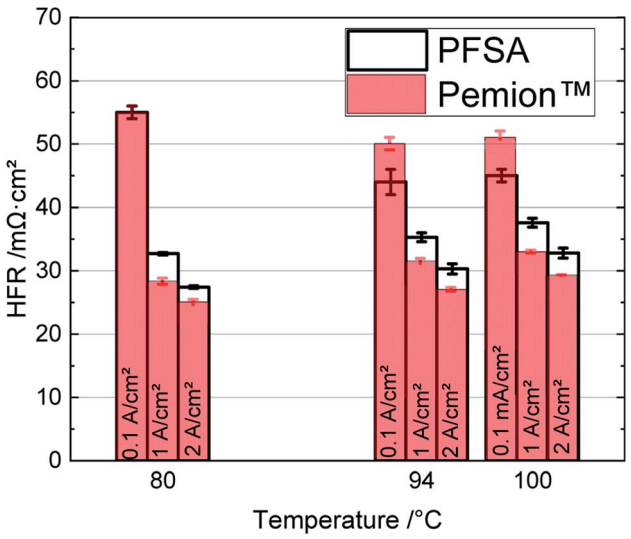

Fig. 7 Direct comparison of the HFRs of Pemion™ MEA and PFSA reference MEA at different current densities (0.1 A cm^{-2}, 1 A cm^{-2}, 2 A cm^{-2}) under operating temperatures 80 °C, 94 °C, and 100 °C.

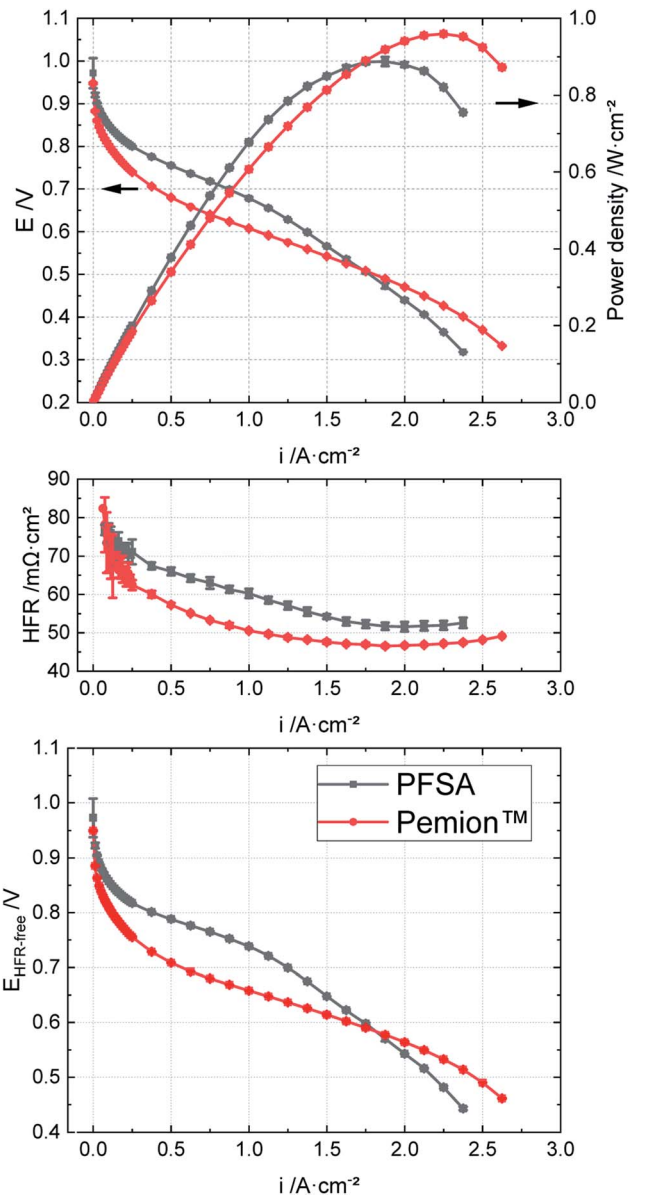

Fig. 8 Polarization behaviours, HFR and HFR-corrected cell voltages of Pemion™ MEA *vs.* PFSA reference at 110 °C under H_2/air, 50% RH, 250 kPa_{abs}.

remains below 0.04 Ω cm² at 100 °C and high current density (2 A cm^{-2}). These results are in accordance with the expectations for hydrocarbon-based ionomers and for SSC-PFSA ionomers as suggested in literature.[14,55]

Very small differences in $E_{HFR\text{-}free}$ with increasing operating temperature from 80 °C to 100 °C are registered for the Pemion™ MEA and PFSA reference (Fig. 6). However, a minor decrease of the potential losses at current densities higher than 2.2 A cm^{-2} can be observed for the PFSA reference with the increasing temperature, while for the Pemion™ MEA this trend cannot be observed.

As next-generation fuel cells might even operate beyond 100 °C, we explored the polarization of both the Pemion™ and SSC PFSA MEAs at 110 °C under H_2/air and 250 kPa_{abs} (Fig. 8). In these tests, the humidity was set to 50% RH to simulate more realistic automotive conditions and to avoid water boiling.[69] Under these conditions, the rated power density of Pemion™ at 110 °C (0.67 W cm^{-2}) is ~20% lower than that of the PFSA reference (0.82 W cm^{-2}), while this gap was significantly higher (50%) at 80 °C (Fig. 2b). Nevertheless, the peak power density of the Pemion™ MEAs (0.96 W cm^{-2}) was ~10% higher than that of the PFSA reference (0.89 W cm^{-2}). This shows that the Pemion™ MEA is a promising candidate for high-temperature operation.

It is striking that the HFRs at 110 °C of both MEAs are higher than at 80 °C (*cf.* Fig. 2b). For example, at 2 A cm^{-2}, the HFR of Pemion™ is ~35% higher than at 80 °C, whereas that of the PFSA is ~40% higher than at 80 °C. The stronger increase in HFR of the PFSA MEA at 110 °C is probably related to the higher thickness and the higher equivalent weight of the PFSA membrane, likely causing stronger membrane dehydration.

The gap of the HFR-corrected cell voltages $E_{HFR\text{-}free}$ between 80 °C and 110 °C is significantly smaller for the Pemion™ MEAs than for the PFSA reference (*cf.* Fig. 2b). This result indicates that the main limitation with high temperature operation for Pemion™ MEAs is a decrease in proton conductivity in the membrane and electrodes. In addition, insufficient water back-diffusion from the cathode to the anode probably leads to membrane and anode dehydration. The lower performance of the PFSA reference may also stem from dehydration of the PFSA ionomer in the electrode.

4 Conclusion

In this work wholly hydrocarbon fuel cells based on Pemion™ (sulfo-phenylated polyphenylene) are reported with a performance that is approaching state-of-the-art PFSA cells under various operation conditions. Under H_2/O_2 with fully humidified gas feeds and ambient pressure, Pemion™ MEAs reach a peak power density (2.1 W cm^{-2}) that is comparable to an optimized short-side chain PFSA reference. In automotive H_2/air conditions with a gas feed humidity of 50% RH and 250 kPa_{abs}, fuel cells comprised of Pemion™ also exhibit comparable performance to that of PFSA-based fuel cells (1.1 W cm^{-2}).

In general, the performance of the Pemion™ cells was found to be more dependent on the humidity of the gas feed than cells with PFSA ionomer. This is argued to be mainly related to a combined effect of lower proton conductivity and slightly lower electrochemical active surface area in the catalyst layer due to a lower (optimal) ionomer content. This leads to a lower performance in the kinetic region despite the similar peak power densities. As typical rated voltages for automotive applications are in this region (0.6 V–0.7 V), the aim of future work should be to reduce the remaining performance gap to PFSA-based cells in this operation window.

Operating automotive fuel cells at elevated temperatures offers several benefits such as reduction in heat exchanger volume and improved system water management. The fuel cells operated from 80 °C to 100 °C showed a negligible impact on performance and small increase in area resistance in both Pemion™ cells and PFSA reference. As hydrocarbon polymers are more tolerant to high temperatures, a ~10% higher peak power density was obtained at 110 °C for the Pemion™ MEA (0.96 W cm^{-2}) compared to the PFSA reference (0.89 W cm^{-2}), showing that the Pemion™ MEA is a promising candidate for high-temperature operation. Studying the transport processes and optimizing the electrodes for hot/dry conditions could yield further improved performance under these conditions.

Previously reported chemical stability data showed that sulfonated phenylated polyphenylenes can withstand 1000 h OCV stress test at exceptionally low degradation rates of 0.16 mV h^{-1},[23] without incorporation of radical scavengers. This excellent stability in combination with the promising performance shown in the present study thereby represents a significant step in the development of next-generation MEAs for hydrogen fuel cells.

Conflicts of interest

Steven Holdcroft is a scientific advisor to Ionomr Innovations Inc.

Acknowledgements

The authors thank Klaus-Dieter Kreuer for the insightful comments and discussion. The authors acknowledge funding from DirectStack (Grant O3ETBO24D), the German-Canadian project FlexCoat/NRC-IRAP 2 + 2 Programme (Grant 01DM19008A), the Natural Science and Engineering Research Council of Canada (NSERC) (Grant CRDPJ529968). The authors acknowledge Carolin Klose and Luca Bohn for the development of the proton conductivity measurement protocol. The authors would like to acknowledge Mark Muggli from 3M for providing SSC-PFSA ionomer and Fumatech for providing SSC-PFSA membrane.

References

1 *Fuel Cells: Selected Entries from the Encyclopedia of Sustainability Science and Technology*, ed. K.-D. Kreuer, Springer, New York, NY, 2013.
2 J. Peron, D. Edwards, A. Besson, Z. Shi and S. Holdcroft, Microstructure–Performance Relationships of sPEEK-Based Catalyst Layers, *J. Electrochem. Soc.*, 2010, **157**, B1230.

3 S. Holdcroft, Fuel Cell Catalyst Layers: A Polymer Science Perspective, *Chem. Mater.*, 2013, **26**, 381–393.
4 K. Goto, I. Rozhanskii, Y. Yamakawa, T. Otsuki and Y. Naito, Development of Aromatic Polymer Electrolyte Membrane with High Conductivity and Durability for Fuel Cell, *Polym. J.*, 2009, **41**, 95–104.
5 K. Miyatake, Membrane Electrolytes, from Perfluorosulfonic Acid (PFSA) to Hydrocarbon Ionomers, in *Fuel Cells: Selected Entries from the Encyclopedia of Sustainability Science and Technology*, ed. K.-D. Kreuer, Springer, New York, NY, 2013.
6 K.-D. Kreuer, Ion Conducting Membranes for Fuel Cells and other Electrochemical Devices, *Chem. Mater.*, 2013, **26**, 361–380.
7 A. Kraytsberg and Y. Ein-Eli, Review of Advanced Materials for Proton Exchange Membrane Fuel Cells, *Energy Fuels*, 2014, **28**, 7303–7330.
8 J. A. Kerres, Design Concepts for Aromatic Ionomers and Ionomer Membranes to be Applied to Fuel Cells and Electrolysis, *Polym. Rev.*, 2015, **55**, 273–306.
9 Japanese New Energy and Industrial Technology Development Organization (NEDO), *Technology Development Roadmap (FCV/Mobile)*, https://www.nedo.go.jp/content/100871975.pdf.
10 U.S. Department of Energy, *Fuel Cell Technical Team Roadmap*, https://www.energy.gov/sites/prod/files/2017/11/f46/FCTT_Roadmap_Nov_2017_FINAL.pdf, accessed December 21, 2020.
11 J. Miyake and K. Miyatake, Fluorine-free sulfonated aromatic polymers as proton exchange membranes, *Polym. J.*, 2017, **49**, 487–495.
12 K. Miyatake and M. Watanabe, Emerging membrane materials for high temperature polymer electrolyte fuel cells: durable hydrocarbon ionomers, *J. Mater. Chem.*, 2006, **16**, 4465.
13 F. Luo, S. Pan and Z. Yang, Recent Progress on Electrocatalyst for High-Temperature Polymer Exchange Membrane Fuel Cells, *Acta Phys.-Chim. Sin.*, 2020, 2009087-0.
14 J. Zhang, Z. Xie, J. Zhang, Y. Tang, C. Song, T. Navessin, Z. Shi, D. Song, H. Wang, D. P. Wilkinson, *et al.*, High temperature PEM fuel cells, *J. Power Sources*, 2006, **160**, 872–891.
15 M. Inaba, T. Kinumoto, M. Kiriake, R. Umebayashi, A. Tasaka and Z. Ogumi, Gas crossover and membrane degradation in polymer electrolyte fuel cells, *Electrochim. Acta*, 2006, **51**, 5746–5753.
16 H. Zhang and P. K. Shen, Recent development of polymer electrolyte membranes for fuel cells, *Chem. Rev.*, 2012, **112**, 2780–2832.
17 L. Gubler, T. Nauser, F. D. Coms, Y.-H. Lai and C. S. Gittleman, Perspective—Prospects for Durable Hydrocarbon-Based Fuel Cell Membranes, *J. Electrochem. Soc.*, 2018, **165**, F3100–F3103.
18 T. Holmes, T. J. G. Skalski, M. Adamski and S. Holdcroft, Stability of Hydrocarbon Fuel Cell Membranes: Reaction of Hydroxyl Radicals with Sulfonated Phenylated Polyphenylenes, *Chem. Mater.*, 2019, **31**, 1441–1449.
19 T. J. G. Skalski, B. Britton, T. J. Peckham and S. Holdcroft, Structurally-defined, sulfo-phenylated, oligophenylenes and polyphenylenes, *J. Am. Chem. Soc.*, 2015, **137**, 12223–12226.
20 M. Adamski, T. J. G. Skalski, B. Britton, T. J. Peckham, L. Metzler and S. Holdcroft, Highly Stable, Low Gas Crossover, Proton-Conducting Phenylated Polyphenylenes, *Angew. Chem., Int. Ed. Engl.*, 2017, **56**, 9058–9061.
21 J. Miyake, R. Taki, T. Mochizuki, R. Shimizu, R. Akiyama, M. Uchida and K. Miyatake, Design of flexible polyphenylene proton-conducting membrane for next-generation fuel cells, *Sci. Adv.*, 2017, **3**, eaao0476.
22 K. Shiino, J. Miyake and K. Miyatake, Highly stable polyphenylene ionomer membranes from dichlorobiphenyls, *Chem. Commun.*, 2019, **55**, 7073–7076.
23 S. Xu, M. Adamski, M. Killer, E. M. Schibli, B. J. Frisken and S. Holdcroft, Sulfo-Phenylated Polyphenylenes Containing Sterically Hindered Pyridines, *Macromolecules*, 2019, **52**, 2548–2559.
24 R. Shimizu, K. Otsuji, A. Masuda, N. Sato, M. Kusakabe, A. Iiyama, K. Miyatake and M. Uchida, Durability of Newly Developed Polyphenylene-Based Ionomer Membranes in Polymer Electrolyte Fuel Cells: Accelerated Stress Evaluation, *J. Electrochem. Soc.*, 2019, **166**, F3105–F3110.
25 L. Gubler, T. Nolte and T. Nauser, Antioxidant Strategies for Hydrocarbon-Based Membranes, *ECS Trans.*, 2018, **86**, 369–379.
26 Y. S. Kim, B. Einsla, M. Sankir, W. Harrison and B. S. Pivovar, Structure–property–performance relationships of sulfonated poly(arylene ether sulfone)s as a polymer electrolyte for fuel cell applications, *Polymer*, 2006, **47**, 4026–4035.
27 K. J. Oberbroeckling, D. C. Dunwoody, S. D. Minteer and J. Leddy, Density of nafion exchanged with transition metal complexes and tetramethyl ammonium, ferrous, and hydrogen ions: commercial and recast films, *Anal. Chem.*, 2002, **74**, 4794–4799.
28 Y. S. Kim, Polymer Electrolytes with High Ionic Concentration for Fuel Cells and Electrolyzers, *ACS Appl. Polym. Mater.*, 2021, **3**, 1250–1270.
29 K. D. Kreuer, On the development of proton conducting polymer membranes for hydrogen and methanol fuel cells, *J. Membr. Sci.*, 2001, **185**, 29–39.
30 K.-D. Kreuer, S. J. Paddison, E. Spohr and M. Schuster, Transport in proton conductors for fuel-cell applications: simulations, elementary reactions, and phenomenology, *Chem. Rev.*, 2004, **104**, 4637–4678.
31 Y. Yang, A. Siu, T. J. Peckham and S. Holdcroft, Structural and Morphological Features of Acid-Bearing Polymers for PEM Fuel Cells, in *Fuel Cells: Selected Entries from the Encyclopedia of Sustainability Science and Technology*, ed. K.-D. Kreuer, Springer, New York, NY, 2013, pp. 55–126.
32 A. Telfah, G. Majer, K. D. Kreuer, M. Schuster and J. Maier, Formation and mobility of protonic charge carriers in methyl sulfonic acid–water mixtures: a model for sulfonic acid based ionomers at low degree of hydration, *Solid State Ionics*, 2010, **181**, 461–465.

33 E. Balogun, M. Adamski and S. Holdcroft, Communication—Non-Fluorous, Hydrocarbon PEMFCs, Generating >1 W cm^{-2} Power, *J. Electrochem. Soc.*, 2020, **167**, 84502.
34 V. Ramani, S. Swier, M. T. Shaw, R. A. Weiss, H. R. Kunz and J. M. Fenton, Membranes and MEAs Based on Sulfonated Poly(ether ketone ketone) and Heteropolyacids for Polymer Electrolyte Fuel Cells, *J. Electrochem. Soc.*, 2008, **155**, B532.
35 A. Strong, B. Britton, D. Edwards, T. J. Peckham, H.-F. Lee, W. Y. Huang and S. Holdcroft, Alcohol-Soluble, Sulfonated Poly(arylene ether)s: Investigation of Hydrocarbon Ionomers for Proton Exchange Membrane Fuel Cell Catalyst Layers, *J. Electrochem. Soc.*, 2015, **162**, F513–F518.
36 T. J. G. Skalski, M. Adamski, B. Britton, E. M. Schibli, T. J. Peckham, T. Weissbach, T. Moshisuki, S. Lyonnard, B. J. Frisken and S. Holdcroft, Sulfophenylated Terphenylene Copolymer Membranes and Ionomers, *ChemSusChem*, 2018, **11**, 4033–4043.
37 J. E. Chae, S. J. Yoo, J. Y. Kim, J. H. Jang, S. Y. Lee, K. H. Song and H.-J. Kim, Hydrocarbon-based electrode ionomer for proton exchange membrane fuel cells, *Int. J. Hydrogen Energy*, 2020, **45**, 32856–32864.
38 E. Balogun, A. O. Barnett and S. Holdcroft, Cathode starvation as an accelerated conditioning procedure for perfluorosulfonic acid ionomer fuel cells, *Journal of Power Sources Advances*, 2020, **3**, 100012.
39 S. Kabir, D. J. Myers, N. Kariuki, J. Park, G. Wang, A. Baker, N. Macauley, R. Mukundan, K. L. More and K. C. Neyerlin, Elucidating the Dynamic Nature of Fuel Cell Electrodes as a Function of Conditioning: An Ex Situ Material Characterization and In Situ Electrochemical Diagnostic Study, *ACS Appl. Mater. Interfaces*, 2019, **11**, 45016–45030.
40 T. van Cleve, G. Wang, M. Mooney, C. F. Cetinbas, N. Kariuki, J. Park, A. Farghaly, D. Myers and K. C. Neyerlin, Tailoring electrode microstructure via ink content to enable improved rated power performance for platinum cobalt/high surface area carbon based polymer electrolyte fuel cells, *J. Power Sources*, 2021, **482**, 228889.
41 R. N. Carter, S. S. Kocha, F. Wagner, M. Fay and H. A. Gasteiger, Artifacts in Measuring Electrode Catalyst Area of Fuel Cells through Cyclic Voltammetry, *ECS Trans.*, 2007, **11**, 403–410.
42 S. Koh, J. Leisch, M. F. Toney and P. Strasser, Structure–Activity–Stability Relationships of Pt–Co Alloy Electrocatalysts in Gas-Diffusion Electrode Layers, *J. Phys. Chem. C*, 2007, **111**, 3744–3752.
43 H. Schulenburg, J. Durst, E. Müller, A. Wokaun and G. G. Scherer, Real surface area measurements of Pt_3Co/C catalysts, *J. Electroanal. Chem.*, 2010, **642**, 52–60.
44 T. Biegler, D. A. J. Rand and R. Woods, Limiting oxygen coverage on platinized platinum; relevance to determination of real platinum area by hydrogen adsorption, *J. Electroanal. Chem. Interfacial Electrochem.*, 1971, 269–277.
45 S. B. Brummer, The use of large anodic galvanostatic transients to evaluate the maximum adsorption of Platinum on formic acid solutions, *J. Phys. Chem.*, 1965, **69**, 562–571.
46 J. Peron, Z. Shi and S. Holdcroft, Hydrocarbon proton conducting polymers for fuel cell catalyst layers, *Energy Environ. Sci.*, 2011, **4**, 1575.
47 F. Huang, T. D. Largier, W. Zheng and C. J. Cornelius, Pentablock copolymer morphology dependent transport and its impact upon film swelling, proton conductivity, hydrogen fuel cell operation, vanadium flow battery function, and electroactive actuator performance, *J. Membr. Sci.*, 2018, **545**, 1–10.
48 M. Hwang, K. Nixon, R. Sun, C. Willis and Y. A. Elabd, Sulfonated pentablock terpolymers as membranes and ionomers in hydrogen fuel cells, *J. Membr. Sci.*, 2021, **104**, 119330.
49 Z. Long, J. Miyake and K. Miyatake, Partially Fluorinated Polyphenylene Ionomers as Proton Exchange Membranes for Fuel Cells: Effect of Pendant Multi-Sulfophenylene Groups, *ACS Appl. Energy Mater.*, 2019, **2**, 7527–7534.
50 Z. Long and K. Miyatake, High-Performance Fuel Cell Operable at 120 °C Using Polyphenlyene Ionomer Membranes with Improved Interfacial Compatibility, *ACS Appl. Mater. Interfaces*, 2021, **13**, 15366–15372.
51 K. C. Neyerlin, H. A. Gasteiger, C. K. Mittelsteadt, J. Jorne and W. Gu, Effect of Relative Humidity on Oxygen Reduction Kinetics in a PEMFC, *J. Electrochem. Soc.*, 2005, **152**, A1073.
52 H. A. Gasteiger, J. E. Panels and S. G. Yan, Dependence of PEM fuel cell performance on catalyst loading, *J. Power Sources*, 2004, **127**, 162–171.
53 K. C. Neyerlin, W. Gu, J. Jorne and H. A. Gasteiger, Determination of Catalyst Unique Parameters for the OxygenReduction Reaction in a PEMFC, *J. Electrochem. Soc.*, 2006, A1955–A1963.
54 Y. Liu, M. W. Murphy, D. R. Baker, W. Gu, C. Ji, J. Jorne and H. A. Gasteiger, Proton Conduction and Oxygen Reduction Kinetics in PEM Fuel Cell Cathodes: Effects of Ionomer-to-Carbon Ratio and Relative Humidity, *J. Electrochem. Soc.*, 2009, **156**, B970.
55 J. Peron, D. Edwards, M. Haldane, X. Luo, Y. Zhang, S. Holdcroft and Z. Shi, Fuel cell catalyst layers containing short-side-chain perfluorosulfonic acid ionomers, *J. Power Sources*, 2011, **196**, 179–181.
56 X. Luo, D. I. Kushner, J. Li, E. J. Park, Y. S. Kim and A. Kusoglu, Anion Exchange Ionomers: Impact of Chemistry on Thin-Film Properties, *Adv. Funct. Mater.*, 2021, **31**, 2008778.
57 H. A. Gasteiger, S. S. Kocha, B. Sompalli and F. T. Wagner, Activity benchmarks and requirements for Pt, Pt-alloy, and non-Pt oxygen reduction catalysts for PEMFCs, *Appl. Catal., B*, 2005, **56**, 9–35.
58 L. Zhang, C. Ma and S. Mukerjee, Oxygen permeation studies on alternative proton exchange membranes designed for elevated temperature operation, *Electrochim. Acta*, 2003, **48**, 1845–1859.
59 R. W. Lindström, A. Oyarce, L. G. Aguinaga, D. Ubeda, M. Ingratta, P. Jannasch and G. Lindbergh, Performance of Phosphonated Hydrocarbon Ionomer in the Fuel Cell

Cathode Catalyst Layer, *J. Electrochem. Soc.*, 2013, **160**, F269–F277.

60 K. Kodama, R. Jinnouchi, T. Suzuki, H. Murata, T. Hatanaka and Y. Morimoto, Increase in adsorptivity of sulfonate anions on Pt (111) surface with drying of ionomer, *Electrochem. Commun.*, 2013, **36**, 26–28.

61 M. P. Soriaga and A. T. Hubbard, Determination of the orientation of adsorbed molecules at solid-liquid interfaces by thin-layer electrochemistry: aromatic compounds at platinum electrodes, *J. Am. Chem. Soc.*, 1982, **104**, 2735–2742.

62 M. K. Sabbe, L. Laín, M.-F. Reyniers and G. B. Marin, Benzene adsorption on binary Pt_3M alloys and surface alloys: a DFT study, *Phys. Chem. Chem. Phys.*, 2013, **15**, 12197–12214.

63 D. Li, H. T. Chung, S. Maurya, I. Matanovic and Y. S. Kim, Impact of ionomer adsorption on alkaline hydrogen oxidation activity and fuel cell performance, *Curr. Opin. Electrochem.*, 2018, **12**, 189–195.

64 I. Matanovic, S. Maurya, E. J. Park, J. Y. Jeon, C. Bae and Y. S. Kim, Adsorption of Polyaromatic Backbone Impacts the Performance of Anion Exchange Membrane Fuel Cells, *Chem. Mater.*, 2019, **31**, 4195–4204.

65 T. Yoshida and K. Kojima, Toyota MIRAI Fuel Cell Vehicle and Progress Toward a Future Hydrogen Society, *Interface Magazine*, 2015, **24**, 45–49.

66 A. Heinzel, J. Roes and H. Brandt, Increasing the electric efficiency of a fuel cell system by recirculating the anodic offgas, *J. Power Sources*, 2005, **145**, 312–318.

67 Q. Yan, H. Toghiani and H. Causey, Steady state and dynamic performance of proton exchange membrane fuel cells (PEMFCs) under various operating conditions and load changes, *J. Power Sources*, 2006, **161**, 492–502.

68 F. A. Uribe, T. E. Springer and S. Gottesfeld, A Microelectrode Study of Oxygen Reduction at the Platinum/Recast-Nafion Film Interface, *J. Electrochem. Soc.*, 1992, **139**, 765–773.

69 A. S. Aricò, A. Di Blasi, G. Brunaccini, F. Sergi, G. Dispenza, L. Andaloro, M. Ferraro, V. Antonucci, P. Asher, S. Buche, *et al.*, High Temperature Operation of a Solid Polymer Electrolyte Fuel Cell Stack Based on a New Ionomer Membrane, *Fuel Cells*, 2010, **10**, 1013–1023.

70 K. D. Kreuer, PFSA membranes and beyond, *Polymers for FuelCells, Energy Storage, and Conversion*, 2017.